

PVP2006-ICPVT-11-93840

FEEDBACK CONTROL OF THE FLUTTER OF A CANTILEVERED PLATE IN AN AXIAL FLOW

Olivier Doaré
UME/ENSTA
91761 Palaiseau cedex
France
Email: olivier.doare@ensta.fr

Thijs Paes
UME/ENSTA
91761 Palaiseau cedex
France
Email: T.M.Paes@student.tue.nl

Michel Ferré
UME/ENSTA
91761 Palaiseau cedex
France
Email: michel.ferre@ensta.fr

ABSTRACT

We investigate the experimental control of the instabilities of a plate in an axial fluid flow. In absence of control, the plate is subjected to a flutter instability once a critical flow velocity is reached. In the present work, the objective of the feedback control is to increase the critical velocity and reduce the vibration amplitude once the flutter has appeared.

Initially, the plate vibration and the action of the piezo-electric sensors is modelled in order to obtain a discrete state-space model of the controlled system. A Galerkin method is used, so that the discrete coordinates are the modal amplitudes of a beam when the flow velocity is zero. The action of the actuator is classically modeled as a momentum acting on the plate. To estimate the validity of the model, frequency response measurements are performed on the system. A good correspondence is found between the model and experiments. Dissipation coefficients are experimentally evaluated.

Next, the feedback control loop design is investigated. As a first approach, a PI controller system is implemented. The controllability and stability limits of the closed loop system are investigated. We choose to implement experimentally this control, as it does not require an overly precise modelisation of the disturbances acting on the plate. Impulse response of the system without flow is performed to investigate the optimal control gain. Other tests are performed to show how the controller works against disturbances from a fluid flow. Despite the strong limitations that have been previously mentioned, some encouraging results have been found. The critical velocity is increased and the amplitude of vibration is lowered.

1 INTRODUCTION

The problem of interaction of axial fluid flows with flexible elongated structures is encountered in situations such as snoring, vibration of reeds in musical instruments, towing cables, pipes and flags. The understanding of the vibration of such structures is of great importance as it is often the source of damage. Two types of vibrations arise in the present study. The former is due to the random forcing of turbulent flow on the structure, the latter is due to the coupling between the structure and the flow, once a critical value of the fluid flow is reached. This instability can be harmful to the structure or its environment (*e.g.* in case of rotor blades or laminar placed fins in heat exchangers, but also pipes conveying fluids, loss of lift force in case of an airplane wing)

The instability conditions of finite length structures in presence of axial flows has received considerable attention in these last decades (see [6,7]). The particular problem of a cantilevered plate in an axial flow has also been investigated [3,5]. A few studies have been reported on the stabilization of these systems by active control [4,1]. The present paper reports a work on the control of the vibration of a finite elastic plate immersed in an axial flow, using piezo-electric actuators and sensors.

In the following section, the modelization of the plate, the actuators and sensors is presented. In section 3 the experimental setup will be presented. Results without flow will be shown to adjust some parameters of the model. The design of a feedback-control loop will be presented in section 4. Then the experimental implementation will be described in section 5. Finally, a dis-

cussion on limitations and possible improvement of the present work will be offered.

2 MODELIZATION OF THE PLATE, ACTUATORS AND SENSORS

The lateral deflection $Y(X, T)$ of a plate of length L and mass per unit length M_s is considered. The axial coordinate is X . A force $F(X, T)$ is acting on the plate. The plate is classically modeled as an Euler-Bernoulli beam, having a flexural rigidity EI . Using the following non-dimensionnal parameters,

$$y = \frac{Y}{L_p}, x = \frac{X}{L_p}, t = \sqrt{\frac{EI}{M_s}} \frac{T}{L_p^2}, f = \frac{L_p^3}{EI} F, \quad (2.1)$$

the equation governing the lateral deflection of the plate is,

$$\frac{\partial^2 y}{\partial t^2} + \frac{\partial^4 y}{\partial x^4} = f(x, t), \quad (2.2)$$

with boundary conditions of a cantilever beam,

$$y(0) = \frac{\partial y}{\partial x} \Big|_{x=0} = 0, \quad \frac{\partial^2 y}{\partial x^2} \Big|_{x=1} = \frac{\partial^3 y}{\partial x^3} \Big|_{x=1} = 0. \quad (2.3)$$

A discrete state-space model is now derived. The displacement and input force are respectively taken of the form,

$$y(x, t) = \sum_{j=1}^{\infty} q_j(t) \phi_j(x), \quad f(x, t) = \sum_{j=1}^{\infty} u_j(t) \phi_j(x). \quad (2.4)$$

Using a truncated sum $j \in [1, N]$, it is possible to express the governing equation of the beam (2.2) in the following form,

$$\begin{bmatrix} \dot{\mathbf{q}}(t) \\ \ddot{\mathbf{q}}(t) \end{bmatrix} = \begin{bmatrix} 0 & Id \\ -K & -C_d \end{bmatrix} \begin{bmatrix} \mathbf{q}(t) \\ \dot{\mathbf{q}}(t) \end{bmatrix} + \begin{bmatrix} 0 \\ \mathbf{u}(t) \end{bmatrix}. \quad (2.5)$$

where Id is the identity matrix and

$$K_{lm} = \int_0^1 \frac{\partial^4 \phi_l(x)}{\partial x^4} \phi_m(x) dx. \quad (2.6)$$

In the present case K is also diagonal because we use the eigenmodes of the beam. We introduce here a diagonal matrix C_d to take into account the dissipation in the system. Its coefficients will be evaluated experimentally in the next section. In case of no dissipation, it is equal to zero.

We introduce now a vector \mathbf{B} , where coefficients quantify the force acting on the beam eigenmodes due to the piezoactuator when its input voltage is 1 [8],

$$\begin{bmatrix} \dot{\mathbf{q}}(t) \\ \ddot{\mathbf{q}}(t) \end{bmatrix} = \begin{bmatrix} 0 & Id \\ -K & -C_d \end{bmatrix} \begin{bmatrix} \mathbf{q}(t) \\ \dot{\mathbf{q}}(t) \end{bmatrix} + \begin{bmatrix} \mathbf{0} \\ \mathbf{B} \end{bmatrix} u(t), \quad (2.7)$$

where,

$$\begin{aligned} B_j u(t) &= \int -E_p d_{31} u(t) b''(x) h \phi_j(x) dx \\ &= -(E_p d_{31} u(t) h) \int b''(x) \phi_j(x) dx. \end{aligned} \quad (2.8)$$

Here, E_p is the electric field in [V/m], d_{31} the piezoelectric constant [m/V], $u(t)$ the applied voltage and b'' is the second derivative of the function b describing the geometry of the piezoactuator in the lateral direction. For a rectangular actuator this function is a sum of two unit step functions; $b(x) = H(x-a) - H(x-b)$, a and b being the left- and right-hand edges of the actuator. After integration by parts, equation (2.8) becomes,

$$B_j u(t) = -E_p d_{31} u(t) h (\phi'_j(b) - \phi'_j(a)). \quad (2.9)$$

This indicates that the effect of the actuators is modeled as two moments, acting on both sides of the actuator. As we use here a single actuator, our configuration is called "asymmetric wafer configuration" [8]. In addition to pure bending, the asymmetric configuration also stretches the plate in lateral direction, see Fig. 2.1. But this effect will be neglected in the following.

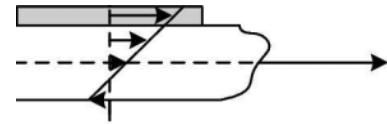


Figure 2.1. Asymmetric wafer actuator configuration

The voltage appearing across the terminals of the sensor will be modeled by the following equation,

$$v(t) = [\mathbf{C} \quad \mathbf{0}] \begin{bmatrix} \mathbf{q}(t) \\ \dot{\mathbf{q}}(t) \end{bmatrix} + d u(t), \quad (2.10)$$

where \mathbf{C} is a vector representing the effect of each modal deformation on the output voltage and d a parameter that quantifies the

direct effect of forcing on the measured voltage. This last parameter is called the transmission effect. To determine the vector \mathbf{C} the same method as for the actuators is used. The output voltage is sought of the form,

$$v(t) = \sum_{k_s=1}^{n_s} \frac{E_p d_{31} h}{C_f} \int_a^b y'' b(x) dx, \quad (2.11)$$

where

$$y''(x, t) = \phi_j''(x) q_j(t) \quad \text{and} \quad (2.12)$$

$$\int_a^b y''(x, t) b_p(x) dx = q_j(t) \int_0^1 \phi_j''(x) b(x) dx. \quad (2.13)$$

The output voltage finally reads,

$$v(t) = \sum_{j=1}^n \frac{E_p d_{31} h}{C_f} (\phi_j'(d) - \phi_j'(c)) q_j(t) = [\mathbf{C}] [\mathbf{q}(t)]. \quad (2.14)$$

3 EXPERIMENTAL SETUP

A plate is immersed in a fluid flow, as represented in Fig. 3.2. Piezoactuators and sensors are fixed on the plate. One pair of ceramics is situated in middle of the plate at 15 cm from the clamp and the other pair is near the clamp at 0.5 cm. Any ceramic can be used as actuator or as sensor. In the present work, only two situations are investigated, both actuation and measurement at clamp, and both actuation and measurement in the middle.

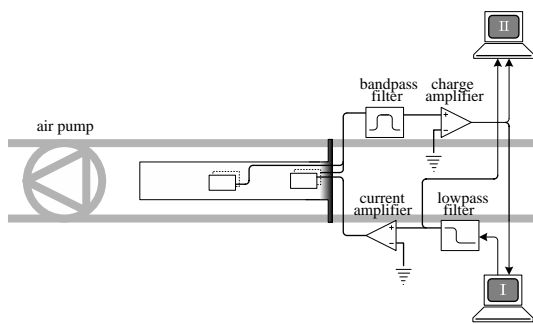


Figure 3.2. Schematic diagram of experimental setup

A PXI computer system with NI LABVIEW software (indicated as 1 in Fig. 3.2) is used to generate an actuation signal. In case of a closed loop for control, the output of one of the sensors is required and is fed into this computer. After the D/A conversion by the NI PXI-system, the actuation signal needs to be

smoother by a low pass filter, having a cut-off frequency of 1 kHz. After this, a power amplifier is used to amplify the actuation signals. A second system with a NI USB data acquisition device is used for data acquisition. This system, indicated as 11 in Fig. 3.2, reads any output signal, which is first filtered by a band pass filter, cutting off frequencies outside the band between 1 Hz and 1 kHz, in order to prevent aliasing. Both actuation and measurement have a sampling rate of 4 kHz.

This setup is now used to determine experimentally the transfer functions of the plate without flow. A chirp-signal is used to excite all frequencies in the band 1 Hz - 400 Hz. Fig. 3.3 shows the measured transfer function when actuating and measuring both at the clamp. Fig. 3.4 shows the measured transfer function when actuating and measuring in the middle of the plate. The modal damping constants can be extracted from these experimental data with the help of a circle fit procedure, which is commonly used for weakly damped systems. These constants are introduced in the matrix \mathbf{C} , see equation (2.5).

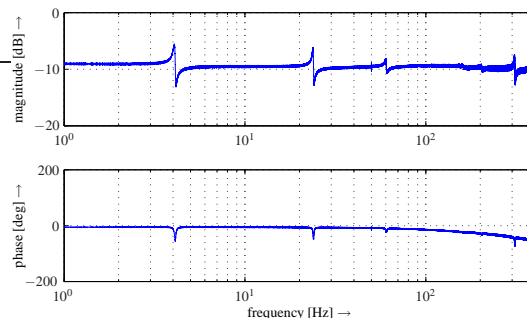


Figure 3.3. Transfer function between forcing and measuring when actuator and sensor are at the clamp.

Fig. 3.5 shows the modeled transfer function between measure and forcing when the piezoactuator and -sensor are at the clamp while Fig. 3.6 shows the same modeled transfer function when the piezoactuator and -sensor are at the middle of the plate. The transmission coefficient d is adjusted so that the experimental and theoretical bode diagrams have the best similarity. Finally, a very good agreement between measured and modelised transfer functions is found. This model will hence be used in the next section to implement feedback control.

4 FEEDBACK-CONTROL DESIGN

The present section considers the implementation of a PID type feedback control. In this so-called closed loop configuration, the controller is designed to modify the response of the system in such a way that the vibrations are reduced, while a

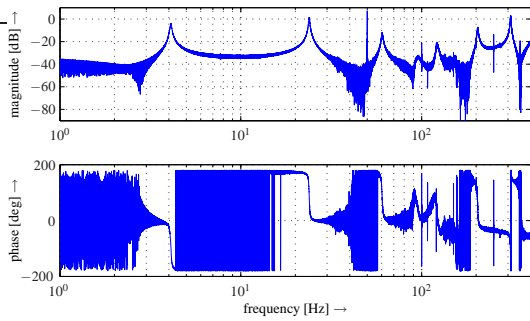


Figure 3.4. Transfer function between forcing and measuring when actuator and sensor are at the middle of the plate.

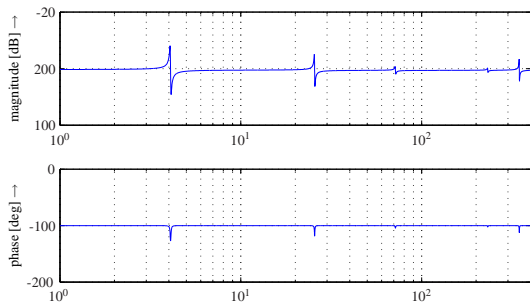


Figure 3.5. Modeled transfer function between forcing and measuring when actuator and sensor are at the clamp.

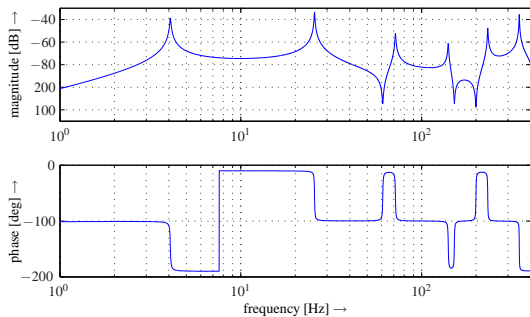


Figure 3.6. Modeled transfer function between forcing and measuring when actuator and sensor are at the middle of the plate.

compromise between performance and stability has to be made. Initially, the behavior of a system with a single control sensor and a single actuator is considered. The same plate with the same piezo electrical elements as in previous section is used. The sensor and actuator that will firstly be used are located at the clamp. The corresponding transfer function to this configuration is plot-

ted in Fig. 3.5. First, the high pass effect in the transducer must be included to the model. This is done by placing a first order high pass filter after the model, which cuts frequencies below 2 Hz. Now the mechanical system in the closed loop situation is considered. The transfer function of the plant is the ratio of the control signal u to the response y , and is denoted as $P(s)$. The transfer function of the feedback controller is analogously defined as the ratio of the error signal e to the excitation of the system u and is denoted as $C(s)$. The error signal is the difference between the reference signal r and the response y . Here $r = 0$ The exit signal y in the closed loop situation reads,

$$y(t) = PC(r - y), \quad (4.15)$$

which can be rewritten in the form,

$$\frac{y}{r} = \frac{PC}{1 + PC}. \quad (4.16)$$

The equivalent block diagram of this type of feedback control is shown in Fig. 4.7.

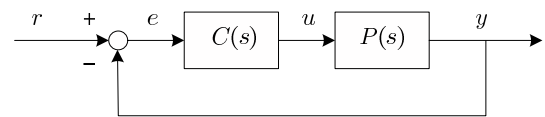


Figure 4.7. Block diagram of the closed loop controller

The design of the controller is now investigated. The vibrations of the plate in presence of fluid flow have been observed to be at lower frequencies than 200Hz. A third order low pass filter with a cut-off frequency at 200 Hz is implemented as a first part of the controller. This filter can be seen as a series of 3 first order filters and reads,

$$C(s) = \left(\frac{1}{\frac{1}{f_{co}} + 1} \right)^3 = \left(\frac{1}{\frac{1}{200} + 1} \right)^3. \quad (4.17)$$

This type of controller is known to become unstable once a critical value of the gain is reached. This arises when there exists frequencies for which the gain of the transfer function between input and output of the closed loop is greater than zero and the phase difference with the zero frequency is greater than 180° . As it appears on Fig. 4.8, representing the transfer function between input and output of the open loop system, the gain margin is equal to 5.9 before instability.

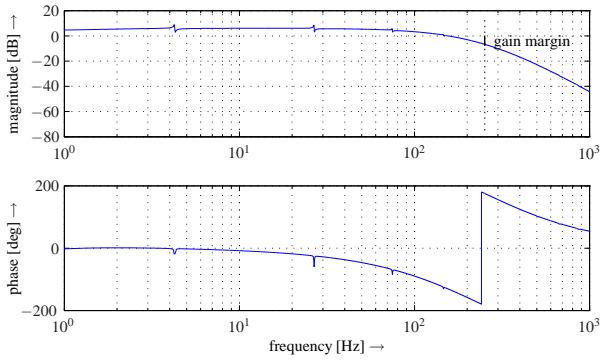


Figure 4.8. Transfer function between input and output of the open loop system.

A stable PID controller with a gain margin of 5.9 has been hence designed. It will be implemented experimentally in the following section.

5 EXPERIMENTAL RESULTS

The theoretical gain margin found in the previous section is hard to estimate experimentally, because many parts of the experimental setup contribute into this gain, namely the current amplifier, the charge amplifier, the AD/DA converters, the gain in the DSP chain and the piezo actuators and sensors. With fixed values of the other gains, we discuss here the adjustment of the gain in the DSP chain, using the impulse response of the closed loop system. On Fig. 5.9 is plotted the variation over time of the output voltage from the sensor and the control signal sent to the actuator during an impulse response test at various gains. It appears on this Figure that when increasing the gain, the maximum peak deflection decreases until a value of 1.5 and increases after.

Moreover, starting at a gain of approximately 3, vibrations are not exponentially damped, a vibration remains, which is due to the instability of the previously described feedback controller. Fig. 5.10 shows the evolution of the maximum peak deflection of the plate, and the RMS value of the deflection of the first five seconds. The optimal value of the gain appears to be around 1.5. In this test, the controller achieves a reduction of 10 dB in the considered period of time between 0 and 4 seconds.

The same controller is now used to reduce the vibrations of the plate in presence of fluid flow. On Fig. 5.11, the amplitude of vibration of the plate is plotted as function of the flow velocity for two different cases, (a), without control, and (b), with control. An hysteresis loop appears, which is due to a subcritical bifurcation. It is well known that this type of instability is subcritical. Before apparition of the instability, the vibrations are due to a forcing by the turbulent flow. A reduction of 5 dB of the RMS value of the measured voltage is observed in presence of control.

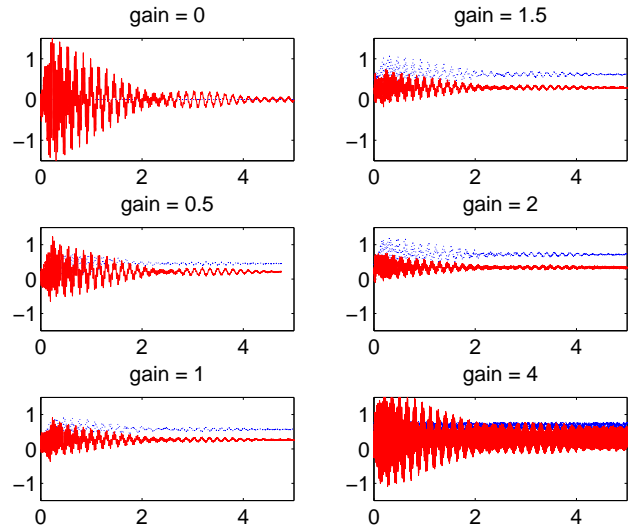


Figure 5.9. Variation over time of input (—) and output (···) of the controller for different values of the gain.

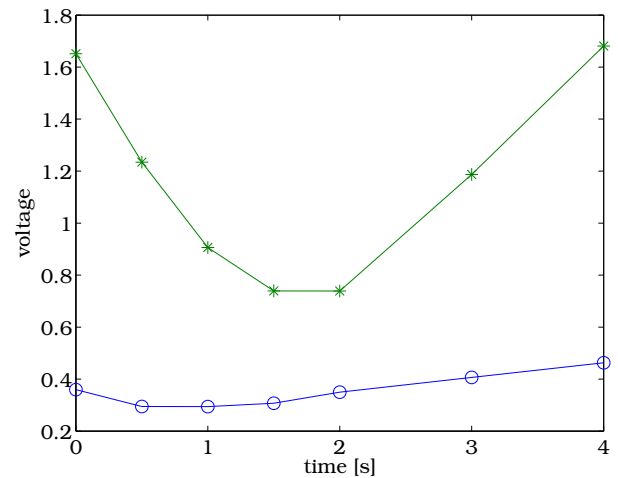


Figure 5.10. Maximum value (*) and RMS value (o) of the input of the controller as function of the gain.

The critical velocity for apparition of the flutter instability is increased by 1% and the amplitude of vibrations once instability saturated is decreased by at least 8 dB¹. The restabilisation of the plate when decreasing the flow velocity appears also earlier,

¹We write here "at least" because the saturation of the charge amplifier has been observed during the vibrations of the plate without control. The value 3.2V appearing on Fig. 5.11 hence might be higher.

by an amount of 0.5%.

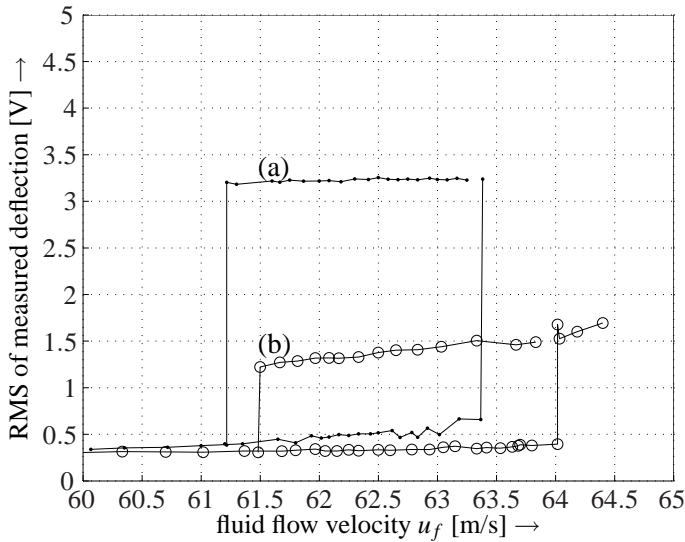


Figure 5.11. RMS amplitude of vibrations as function of the velocity of the flow; (a), without control; (b), with control.

The feedback control we implemented in the present work has been proven to be efficient in reducing the vibrations of the plate, both before and after flutter instability. However, the critical velocity has been increased by a non-significant amount (1%). Moreover, this shift may be due to the random vibrations reduction, which, in case of subcritical bifurcation, may prevent the jump from one stable branch to another.

6 FUTURE IMPROVEMENTS

It is expected that using H_2 or H_∞ control types will allow to push further the instability threshold as they can be designed to maintain the system on the unstable equilibrium state $y(x, t) = 0$. To achieve this control, a good comprehension and a fine modelization of the effect of flow is needed. The flow effect is classically taken into account by adding a centrifugal term and a Coriolis term to the beam equation (2.2), which then reads,

$$\frac{\partial^2 y}{\partial t^2} + u_f^2 \frac{\partial^2 y}{\partial x^2} + \frac{\partial^4 y}{\partial x^4} + 2\beta^{1/2} u_f \frac{\partial^2 y}{\partial x \partial t} = f(x, t), \quad (6.18)$$

where,

$$\beta = \frac{M_f}{M_f + M_s}, \quad u_f = \sqrt{\frac{M_f}{EI}} L_p U_f, \quad (6.19)$$

are the mass ratio and the non-dimensional velocity respectively. The precise evaluation of the parameter M_f represents the main difficulty of the modelization, see [2] in the present proceedings as an example of the fact that many improvements are still to be done. Taking here,

$$M_f = \frac{\pi \rho B}{4}, \quad (6.20)$$

as in [3,5] gives good qualitative behavior for the variation of the critical velocity as function of the other parameters, but conducted to errors that are enough to prevent an efficient implementation of optimal or robust control.

7 CONCLUSION

The feedback control of the vibrations of a plate in an axial flow has been presented. The modelization of the plate vibrations, of the forcing and of measuring by piezo-electric components have been derived. This model has been proven to be accurate and has been used as a basis for the design of a stable feedback loop. Finally, a reduction of 5 dB of the vibration of the plate due to turbulent flow and of 8 dB of the vibration at flutter instability have been achieved. The instability threshold has been increased by only a small amount. Future improvements may include a better modelization of fluid flow effect on the plate and the implementation of H_2 or H_∞ control.

REFERENCES

- [1] H. Doki, K. Hiramoto, and R.E. Skelton. Active control of cantilevered pipes conveying fluids with constraints on input energy. *Journal of Fluids and Structures*, 12:615–628, 1998.
- [2] C. Elloy, C. Souillez, and L. Schouveiler. Flutter of a rectangular cantilevered plate. In *6th FSI, AE & FIV+N Symposium*, Vancouver, 2006.
- [3] L. Huang. Flutter of cantilevered plates in axial flow. *Journal of Fluids and Structures*, (9):127–147, 1995.
- [4] S. Kaneko and K. Hirota. A study on active control of leakage flow induced vibrations. In *1st International Conf. on Motion and Vibration Control*, pages 1135–1140, 1992.
- [5] C. Lemaître, P. Hémon, and E. de Langre. Instability of a long ribbon hanging in axial air flow. *Journal of Fluids and Structures*, 7:913–925, 2005.
- [6] M. P. Paidoussis. *Fluid-structure Interactions. Slender Structures and Axial Flow*, volume 1. Academic Press, 1998.
- [7] M. P. Paidoussis. *Fluid-structure Interactions. Slender Structures and Axial Flow*, volume 2. Academic Press, 2004.
- [8] A. Preumont. *Vibration Control of Active Structures*. Kluwer Academic Publishers, Dordrecht, 1996.